EFFECT OF ILLITE PARTICLE SHAPE ON CESIUM SORPTION

Pavol Rajec,[1] Vladimír Šucha,[2] Dennis D. Eberl,[3] Jan Środoń,[4] and Françoise Elsass[5]

[1] Department of Nuclear Chemistry, Comenius University, Mlynská dolina, 842 15 Bratislava, Slovakia
[2] Department of Geology of Mineral Deposits, Comenius University, Mlynská dolina, 842 15 Bratislava, Slovakia
[3] U.S. Geological Survey, 3215 Marine Street, Boulder, Colorado 80303, USA
[4] Institute of Geology, Polish Academy of Sciences, Senacka 1, Krakow, Poland
[5] INRA, Station de Science du Sol, Route de St. Cyr, 78026 Versailles, France

Abstract—Samples containing illite and illite-smectite, having different crystal shapes (plates, "barrels", and filaments), were selected for sorption experiments with cesium. There is a positive correlation between total surface area and Cs-sorption capacity, but no correlation between total surface area and the distribution coefficient, K_d. Generally K_d increases with the edge surface area, although "hairy" (filamentous) illite does not fit this pattern, possibly because elongation of crystals along one axis reduces the number of specific sorption sites.

Key Words—Cesium Sorption, Distribution Coefficient, Illite, Particle Shape.

INTRODUCTION

The behavior of cesium in natural systems, including its interactions with inorganic materials and with the biosphere, must be understood if atomic energy is to be used safely. Clay minerals, which are common at the earth's surface, are good sorbents of cesium (*e.g.,* Sawhney, 1972; Cornell, 1993). The preferential sorption of Cs^+ by clays is related predominantly to its low hydration energy (Coleman *et al.,* 1963; Sawhney, 1964; Kittrick, 1966; Eberl, 1980; Komarneni and Roy, 1988). Cations with low hydration energy, such as K^+, NH_4^+, Rb^+, and Cs^+ may cause high-charge smectite and vermiculite interlayers to dehydrate and collapse, thereby fixing these ions in the interlayer (Komarneni and Roy, 1988).

Generally, the tendency towards fixation by swelling clays is related directly to layer charge and cation-exchange capacity (CEC). However, in very dilute Cs^+ solutions, illite, which has a smaller cation-exchange capacity than vermiculite, sorbs more Cs^+ than vermiculite (Jacobs and Tamura, 1960; Tamura and Jacobs, 1960). This specificity of illite for Cs has been related to the presence of frayed edges (Gaudette *et al.,* 1966) which have sites where the Cs is adsorbed preferentially, or to "weak force fixation", whereby diffuse charges around illite crystals attract Cs^+ most strongly because it is the least strongly hydrated cation (Eberl, 1980). Whatever the origin, Cs-specific sites represent a maximum of 2% of the total CEC of illite (Klobe and Gast, 1970; Cremers *et al.,* 1988; Cornell, 1993).

Illite is used widely for Cs-sorption experiments, but detailed information about the crystal chemistry, origin, particle-size distribution, and particle shape of the illite used in these experiments, often is not reported. An illite particle, as defined in this paper, is equivalent to the fundamental particle defined by Na-

deau *et al.* (1985). Fundamental illite particles are the smallest physically separable, non-expanding particles that contain 2:1 layers bound by fixed potassium cations. These illite particles may occur both as separate particles and as stacks of particles having expandable interfaces (mixed-layer illite-smectite crystals or MacEwan crystallites; Środoń *et al.,* 1990). The maximum proportion of expandable interfaces is expressed as maximum expandability ($\%S_{MAX}$), and is a function of the mean particle thickness (T, where $\%S_{MAX} = 100/T$; Środoń *et al.,* 1992). Expandability also can be measured by X-ray diffraction (XRD) of ethylene glycol-saturated samples, but this technique is affected strongly by the shapes of fundamental illite particles (Środoń and Elsass, 1994; Šucha *et al.,* 1996); therefore XRD techniques were not applied to our samples. In this paper we compare the sorptive properties for Cs^+ of a variety of illites and illite-smectites having different particle shape and thickness. The first goal is to document that different illites may sorb Cs^+ differently, and the second is to determine what illite characteristics control Cs^+ sorption.

MATERIALS AND METHODS

Illite and illite-smectite samples with particles having different shapes (Figure 1) were selected for sorption experiments. The term "illite" is used hereafter to reference either the illite or illite-smectite samples. Selection was based on transmission electron micrographs of ultrathin sections and of dried suspensions. The ultrathin sections were used to document differences between barrel-shaped and platy particles. Maximum expandabilities calculated from transmission electron microscopy (TEM) measurements of mean T are listed in Table 1.

Two samples, one from Le Puy, France (Gabis, 1963), and the other from Muloorina, Australia (Norrish and Pickering, 1983), have particles with barrel-
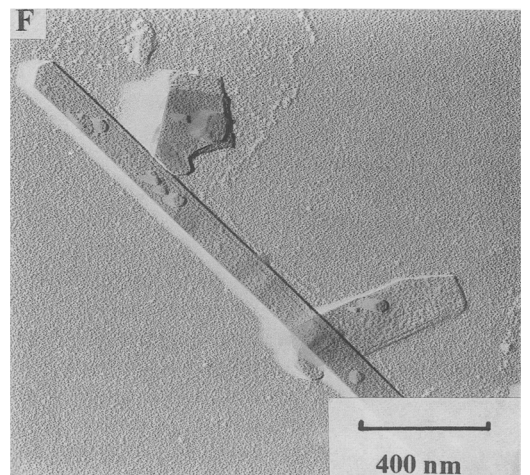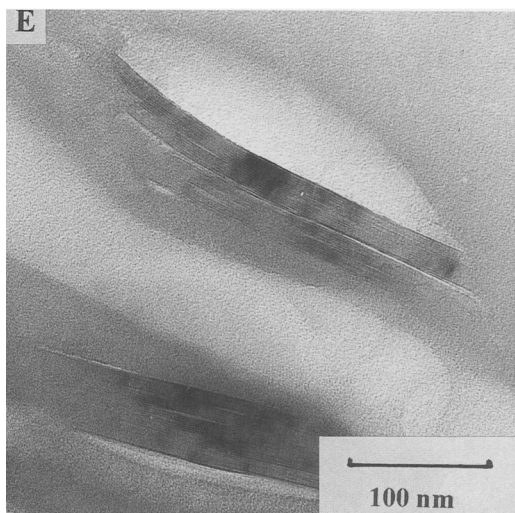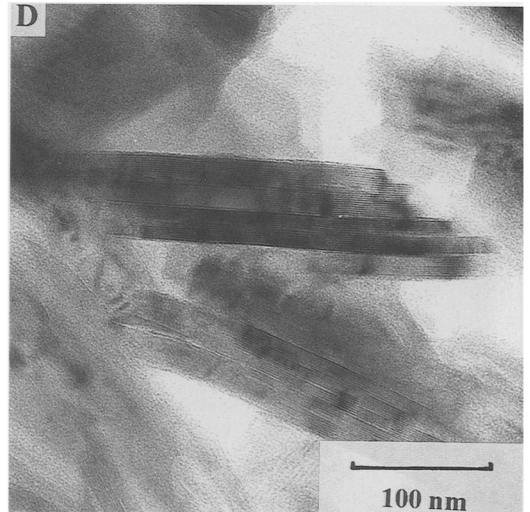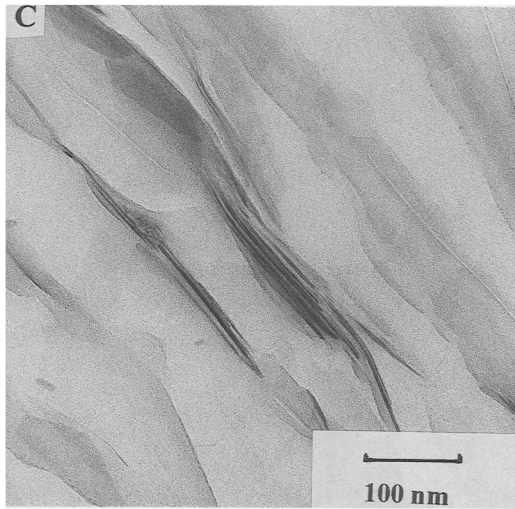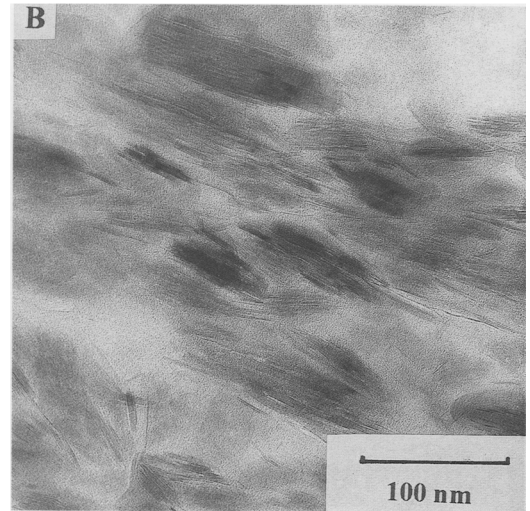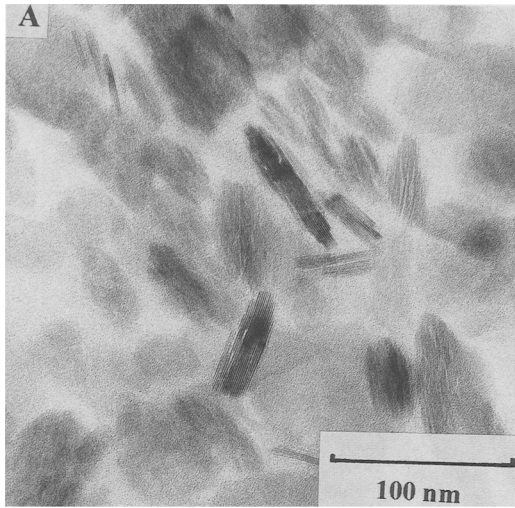
Table 1. Characteristics of samples used for the sorption experiments.

Sample	Shape	Fix	T_{FIX}	$\%S_{MAX}$	TSA	A, B	r	ESA
DVS	Plates	0.50	2.4	42	350		160	0.005
Le Puy	"Barrels"	0.64	3.6	28	233		26	0.029
Muloorina	"Barrels"	0.66	4.0	25	208		23	0.033
L-2A-2	"Hairy"	0.78	8.0	13	108	560, 99		0.009
RM30	Plates	0.80	10.0	10	83		217	0.004
SG4	Plates	0.84	16.6	6	50		427	0.002

FIX = fixed cations content per $O_{10}(OH)_2$; T_{FIX} = mean particle thickness (in nm) calculated from fixed cations; $\%S_{MAX}$ = maximum expandability calculated from T_{FIX}; TSA = total surface area in m^2/g calculated from T_{FIX}; A, B = particle length and width (in nm) along axis a and b, respectively; r = particle radius (in nm); ESA = edge surface area in m^2/g calculated from r or A and B.

like shapes. Both are ferruginous illite of Oligocene age that originated in alkaline lakes. The third sample is a "hairy" (filament-shaped) illite (L-2A-2) from a Triassic sandstone (Poland) with particle elongated parallel to one crystallographic axis. Chemical data and TEM images for "hairy" illite used in this study were obtained from Środoń and Elsass (1994) who describe a different sample, L-2A-1, from the same location. Two samples of platy habit (RM30 and SG4) of hydrothermal origin (Eberl *et al.*, 1987) differ mainly in particle thickness and polytype. Sample DVS, from the Dolna Ves hydrothermal deposit in Slovakia (Šucha *et al.*, 1992), contains large, very thin plates.

Mean particle thicknesses (Table 1) were calculated from illite chemical compositions according to T = $0.9542 - 1.0676$FIX (Środoń *et al.*, 1992), where FIX = fixed-cation content per $O_{10}(OH_2)$. Particle length, width, and/or radius were measured from TEM images for the Muloorina and L-2A-2 samples using 120 and 155 particles, respectively. Other particle-size data were obtained from Środoń *et al.* (1992) and Środoń and Elsass (1994).

Sorption experiments used the <2-μm size fractions treated with sodium acetate and sodium-dithionite, and then exchanged with 1 M NaCl (Jackson, 1975) prior to size fractionation. Excess salts were removed by dialysis. The sorption experiments were performed using 50 mg of sample (dried at 60°C) placed into polyethylene tubes with 5 mL of solution having different Cs concentrations ($0.01–5 \times 10^{-6}$ M) and containing ^{137}Cs tracer. $NaNO_3$ (0.01 M) was used as a background electrolyte. The suspensions were shaken for 2 h in end-over-end shakers (Staunton and Roubaud, 1997). One mL aliquots were taken for Cs activity determination after centrifugation at 12,000 rpm. Activity was measured in a well-type NaI detector (Modumatic Packard, USA). Loss of activity due to sorption on illites was determined by comparison with an aliquot taken prior to exchange.

Distribution coefficients (K_d) were calculated using $K_d = (n_o - n)V/nm$, where n_o and n are count rates of initial and equilibrated solutions, respectively, m is mass of sample in mg, and V is volume of solution in mL. The sorption uptake (Γ) of Cs was calculated for each concentration from the formula $\Gamma = c_{eq}K_d$ [mol kg^{-1}], where c_{eq} is the Cs concentration after equilibration. The maximum Γ for each sample represents the sorption capacity of each sample for Cs. Neither the kinetics nor the reversibility of the sorption was studied. A short exchange period of 2 h avoided interference from a slow reaction known as the second stage of the sorption reaction (Cornell, 1993).

RESULTS AND INTERPRETATIONS

Distribution coefficients (K_d), plotted as a function of equilibrated Cs concentration (c_{eq}), are given in Figure 2. Three trends for the six samples are evident. One trend, represented by the Le Puy and Muloorina samples (barrel-shaped), indicates a very steep increase in K_d with a decrease in Cs concentration. A trend showing a gentle increase in K_d with a decrease in Cs concentration is represented by "hairy" illite L-2A-2, and platy illites RM 30 and SG4. The lowest K_d was obtained for "hairy" illite. Sample DVS has a K_d similar to that of Le Puy and Muloorina illites at higher Cs concentrations, but the K_d is nearly stable at lower Cs concentrations (varying between 600–700), and falls between the other two trends.

Where Cs uptake of the illites is plotted against equilibrated concentrations (Figure 3), different relations are observed for different samples. Sample DVS (very thin plates) has the highest sorption capacity. The Le Puy and Muloorina (barrel-shaped illites) have significantly lower capacity, followed by RM 30 and SG4 (platy illites). The lowest sorption was measured for L-2A-2 illite ("hairy" illite).

Cs-sorption capacity should be related closely in illitic minerals to the CEC, which is a function of the

←

Figure 1. TEM micrographs of illites from ultrathin sections (A) Muloorina, (B) Le Puy, (C) DVS, (D) RM30, (E) SG4, and (F) Pt-shadowed (L-2A-2) samples.
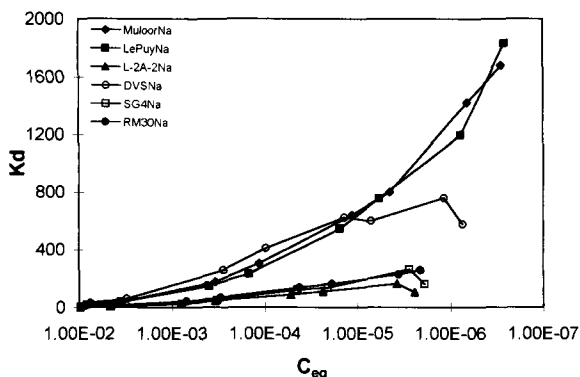
Figure 2. Relation between K_d and logarithm of equilibrated Cs concentration of six studied samples.

Figure 4. Relation between sorption capacity and total surface area calculated from fixed cations of illites.

total surface area of the sample and the 2:1 layer charge. Total surface area (TSA) includes basal interfaces between (non-expanding) illite fundamental particles (Nadeau *et al.*, 1985) and the edges of illite particles. TSA can be measured by the EGME (ethylene glycol monoethyl ether) technique or calculated from the mean thickness (T) of the particles (TSA = 100/0.12T, Środoń *et al.*, 1992). TSA values calculated from T are listed in Table 1. TSA is equivalent to maximum expandability ($\%S_{MAX}$) since both parameters are calculated from T. The relation between measured sorption capacity and total surface area (Figure 4) shows a positive correlation for all of the samples except for the "hairy" illite. The value for the "hairy" illite is below that for the other samples. The plot shows for most of the samples that the maximum sorption capacity can be expressed as a function of the total surface area of illite and/or illite-smectite. Where the same TSA data were plotted *versus* K_d, no clear relation was found (Figure 5). Evidently, K_d is related to other factors.

Since K_d expresses Cs selectivity, the value should be a function of the number of selective sites on illite
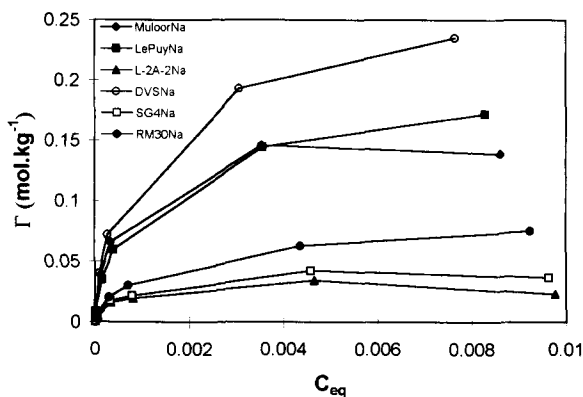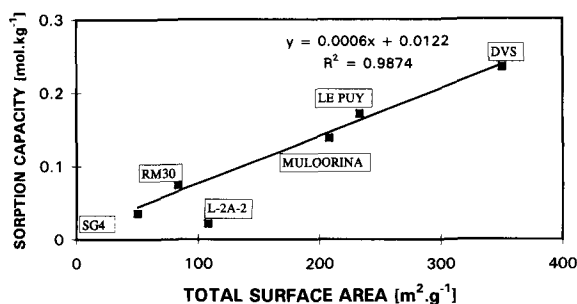
particles. If selective sites correspond to the number of frayed edges (according to the frayed-edge theory of Gaudette *et al.*, 1966), then selectivity may be related to edge surface area. To test this assumption, we calculated edge surface area (ESA) from TEM data by assuming that the platy particles (RM30, SG4, DVS) and the barrel-like particles (Le Puy, Muloorina) have cylindrical shapes. The relationship is ESA (area/unit mass) = $2\pi rT/\pi r^2 Td$ = 2/rd, where r is particle mean radius, T is mean thickness, and d is density of the illite. Assuming d = 2.6 g cm^{-3} (Środoń *et al.*, 1992), then ESA = 0.77/r. Approximation of a cylindrical shape cannot be used for "hairy" illite (L-2A-2) because the dimensions along the *a* and *b* axes (A and B) are very different. For this particular sample ESA = 2(A + B)T/ABTd = 0.77(A + B)/AB.

The data used for the ESA calculations are listed in Table 1. Figure 6 shows a plot of ESA *versus* K_d, which displays a positive correlation for all samples except for the "hairy" illite (L-2A-2), which falls well below the general trend. Thus, we conclude that the selectivity of illite for Cs is related to the edge surface area.

The different behavior of "hairy" illite may be related to its unusual shape. All crystals in this sample are elongate along one axis (length:width = 6:1) so that the sample has significantly fewer sorption sites available along the particle width, which may have a different number of sites suitable for Cs sorption. We speculate that the elongated shape of the particles will
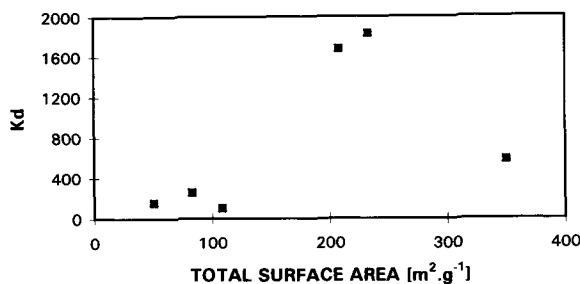

Figure 3. Sorption uptake plotted against the equilibrated Cs concentration.

Figure 5. K_d as a function of total surface area calculated from fixed cations of illites.
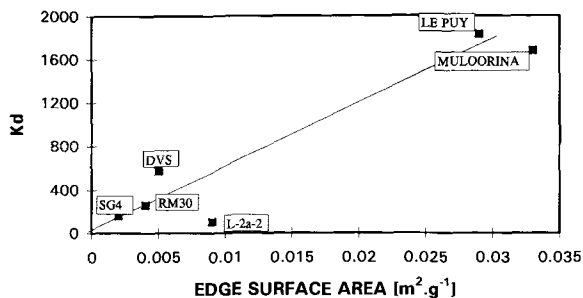
Figure 6. Plot of K_d versus edge surface area of illite particles.

reduce the amount of specific sites, and perhaps explain the lower distribution coefficient. Other samples analyzed have A:B ratios between 1:1 and 1:3. The barrel-like particles have specific kink sites (Figure 7) that may also increase K_d significantly.

CONCLUSIONS

The K_d of illites depends strongly on their edge surface area which may be related to frayed edges. The K_d is unrelated to the total surface area of illites, which includes both basal surfaces of illite fundamental particles and edge surface area. The highest K_d was found for illites with "barrel" shapes (Muloorina, Le Puy). Sorption capacity of illites is related closely to their total surface area which is, in the most cases, equivalent to maximum expandability, which is a function of the mean thickness. The poor sorption properties of "hairy" illite may be related to elongation of crystals
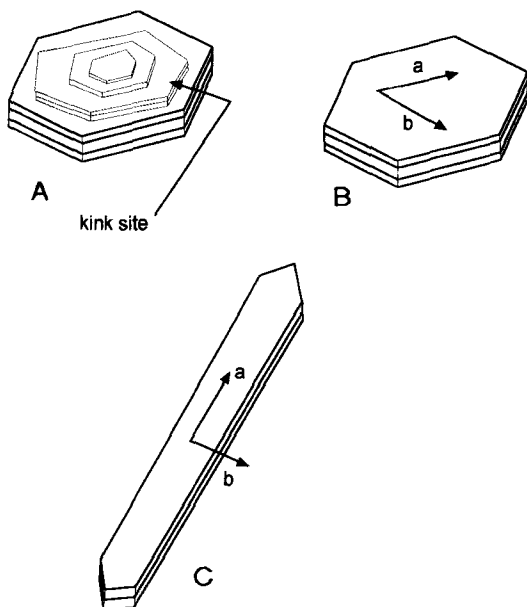

Figure 7. Three different shapes of illite particles used in the study. (A) barrel-like illite, (B) platy illite, (C) "hairy" illite.

along one axis, which may reduce the number of Cs specific sites.

REFERENCES

Coleman, N.T., Craig, D., and Lewis, R.J. (1963) Ion-exchange reactions of cesium. Soil Science Society of America Proceedings, 27, 287–289.

Cornell, R.M. (1993) Adsorption of cesium on minerals: A review. Journal of Radioanalytical and Nuclear Chemistry, Articles, 171, 483–500.

Cremers, A., Elsen, A., De Preter, P., and Maes, A. (1988) Quantitative analysis of radiocaesium retention in soils. Nature, 335, 247–249.

Eberl, D.D. (1980) Alkali cation selectivity and fixation by clay minerals. Clays and Clay Minerals, 28, 161–172.

Eberl, D.D., Środoń, J., Lee, M., Nadeau, P.H., and Northrop, H.R. (1987) Sericite from the Silverton caldera, Colorado: Correlation among structure, composition, origin and particle thickness. American Mineralogist, 72, 914–934.

Gabis, V. (1963) Etude mineralogique et geochimique de la serie sedimentaire oligocene du Velay. Bulletin Societe Francaise de Mineralogie et Cristallographie, 86, 315–354.

Gaudette, H.E., Grim, R.E., and Metzger, C.F. (1966) Illite: A model based on the sorption behaviour of cesium. American Mineralogist, 51, 1649–1656.

Jackson, M.L. (1975) Soil Chemical Analysis—Advanced Course. By author, Madison, Wisconsin, 389 pp.

Jacobs, D.G. and Tamura, T. (1960) The mechanism of ion fixation using radio-isotope techniques. Transaction of the International Congress of Soil Science, 7, Madison, 1960, International Society of Soil Science, Elsevier, Amsterdam, 206–214.

Kittrick, J.A. (1966) Forces involved in ion fixation by vermiculite. Soil Science Society of America Proceedings, 30, 801–803.

Klobe, B. and Gast, R.G. (1970) Conditions affecting cesium fixation and sodium entrapment in hydrobiotite and vermiculite. Soil Science Society of America Proceedings, 34, 746–750.

Komarneni, S. and Roy, R. (1988) A cesium selective ion sieve made by topotactic leaching. Science, 239, 1286–1288.

Nadeau, P.H., Wilson, M.J., McHardy, W.J., and Tait, J.M. (1985) The conversion of smectite to illite during diagenesis: Evidence from some illitic clays from bentonites and sandstones. Mineralogical Magazine, 49, 393–400.

Norrish, K. and Pickering, G.J. (1983) Clay Minerals. In Soils: An Australian Viewpoint. Division of Soils, CSIRO, Academic Press, Melbourne, 281–308.

Sawhney, B.L. (1964) Sorption and fixation of microquantities of Cs by clay minerals: Effect of saturating cations. Soil Science Society of America Proceedings, 28, 183–186.

Sawhney, B.L. (1972) Selective sorption and fixation of cations by clay minerals: A review. Clays and Clay Minerals, 20, 93–100.

Środoń, J. and Elsass, F. (1994) Effect of the shape of fundamental particles on XRD characteristics of illitic minerals. European Journal of Mineralogy, 6, 113–122.

Środoń, J., Elsass, F., McHardy, W.J., and Morgan, D.J. (1992) Chemistry of illite-smectite inferred from TEM

measurements of fundamental particles. *Clay Minerals,* **27,** 137–158.

Staunton, S. and Roubaud, M. (1997) Adsorption of ^{137}Cs on montmorillonite and illite: Effect of charge compensing cation, ionic strength concentration of Cs, K and fulvic acid. *Clays and Clay Minerals,* **45,** 251–260.

Šucha, V., Kraus, I., Mosser, C., Hroncová, Z., Soboleva, K.A., and Širáňová, V. (1992) Mixed-layer illite/smectite from the Dolná Ves hydrothermal deposit, The Western Carpathians, Kremnica Mts. *Geologica Carpathica-Series Clays,* **43,** 13–19.

Tamura, T. and Jacobs, D.G. (1960) Structural implications in cesium sorption. *Health Physics,* **2,** 391–398.